

Supporting Information

A green electrochemical transformation of inferior coals to crystalline graphite for stable Li ion storage

Zhenglu Zhu,^a Haibin Zuo,^{*a} Shijie Li,^a Jiguo Tu,^a Wei Guan,^a Wei-Li Song,^{*b} Jun Zhao,^a

Donghua Tian^a and Shuqiang Jiao^{*a}

^a *State Key Laboratory of Advanced Metallurgy, University of Science and Technology Beijing, 100083, P R China.*

^b *Institute of Advanced Structure Technology, Beijing Institute of Technology, Beijing 100081, P R China*

^{*} *E-mails: zuohaibin@ustb.edu.cn (H Zuo), weilis@bit.edu.cn (W.L. Song), sjiao@ustb.edu.cn (S Jiao)*

Table S1. Proximate (dry basis, db) and elemental (dry ash-free basis, daf) analyses of KL coal.

	KL-RAW	KL-HPC
Proximate analyses(wt%, db)		
Ash	10.37	0.49
Volatile matter	32.2	49.51
Elemental analyses(wt%, daf)		
Carbon	83.25	82.49
Hydrogen	5.37	5.50
Nitrogen	1.8	4.31
sulfur	1.09	0.55
Oxygen	8.49	7.15

Table S2. Abbreviations of samples under different conditions.

Sample	Abbreviation
KL RAW coal	RC
HyperCoal	HPC
850°C-2.6V-10h	EG1
900°C-2.6V-10h	EG2
950°C-2.2V-10h	EG3
950°C-2.4V-10h	EG4
950°C-2.6V-2h	EG5
950°C-2.6V-4h	EG6
950°C-2.6V-6h	EG7

Table S3. The carbon recovery after electrolysis of 0.85g HPC in CaCl₂ under different conditions

Electrode potential	Electrolysis time	Carbon recovery
no potential	20	91%
EG1	10 h	68%
EG2	10 h	60%
EG3	10 h	65%
EG4	10 h	62%
EG5	2 h	79%
EG6	4 h	75%
EG7	6 h	52%

* The decrease in yield is attributed to the removal of oxygen, the drop of HPC into the molten salt during electrolysis and the mass loss during the washing process.

Table S4. Structural parameters of HPC and synthetic graphite structure EG7.

samples	BET surface Area (m²/g)	Total pore volume (cc/g)	Mesopore Volume (cc/g)	Mesopore diameter (nm)
HPC	25.454	/	0.07402	2.191
EG7	131.180	0.1092	0.0605	3.407

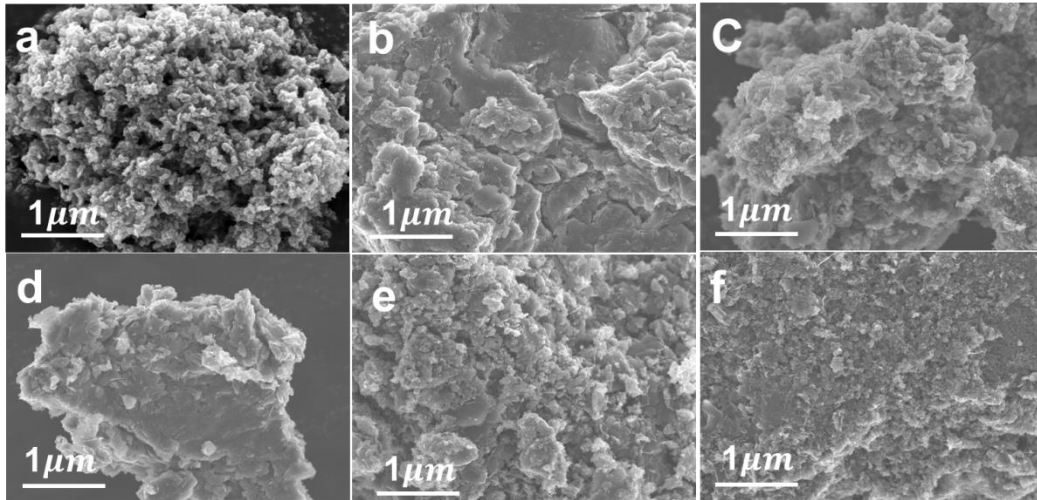


Fig. S1 SEM images of the obtained products at different conditions in CaCl_2 . (a) EG1. (b) EG2. (c) EG3. (d) EG4. (e) EG5. (f) EG6.

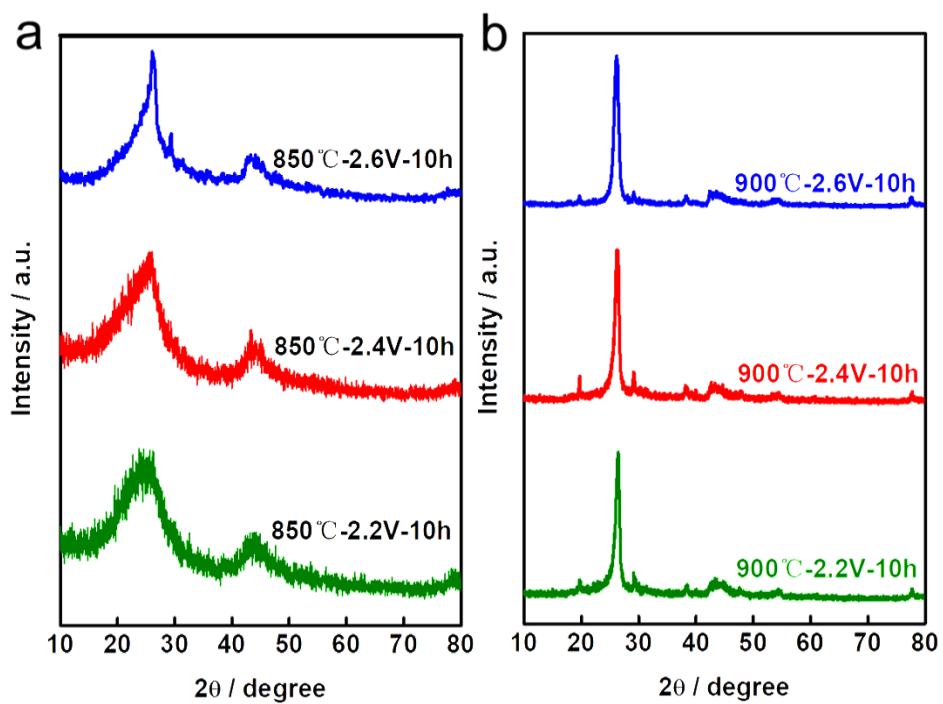


Fig. S2 XRD patterns of electrolyzed HPC under different voltages as indicated at 850 °C and 900 °C.

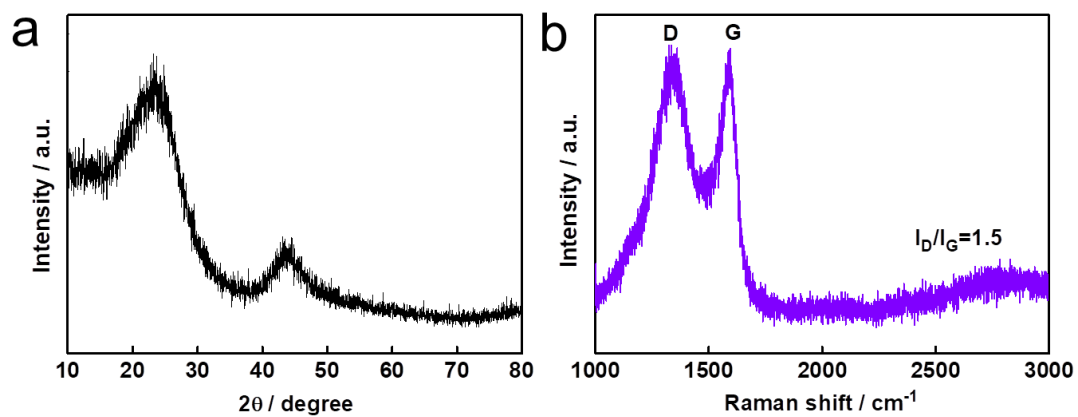


Fig. S3 (a) XRD pattern and (b) Raman spectra of pyrolytic HPC at 850°C for 20 h.

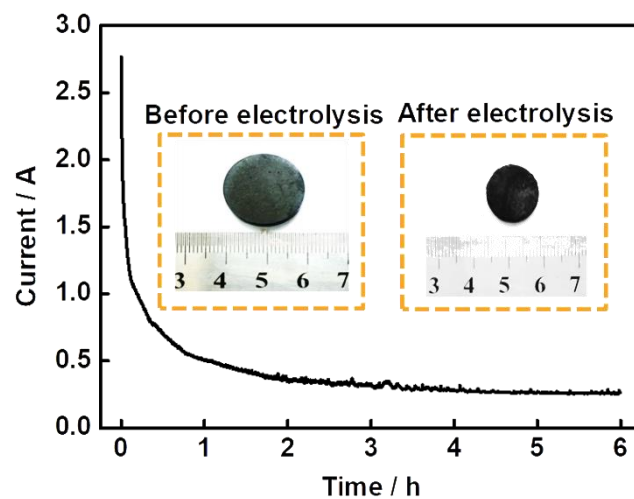


Fig. S4 Current response under 2.6V at 950°C for 6h.

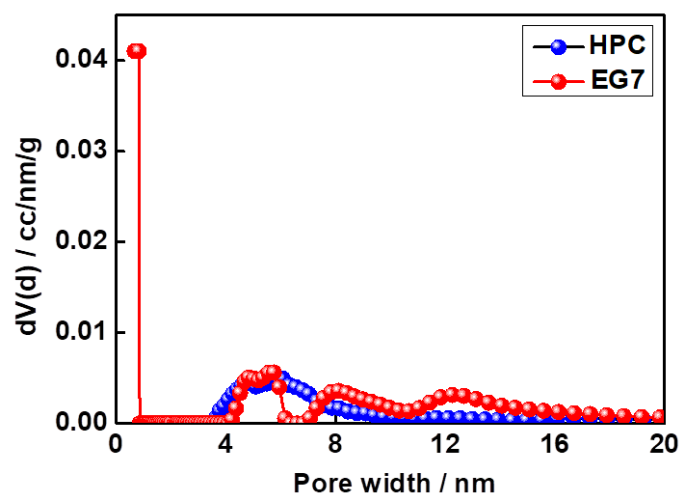


Fig. S5 Pore size distribution (PSD) curves of HPC and EG7.

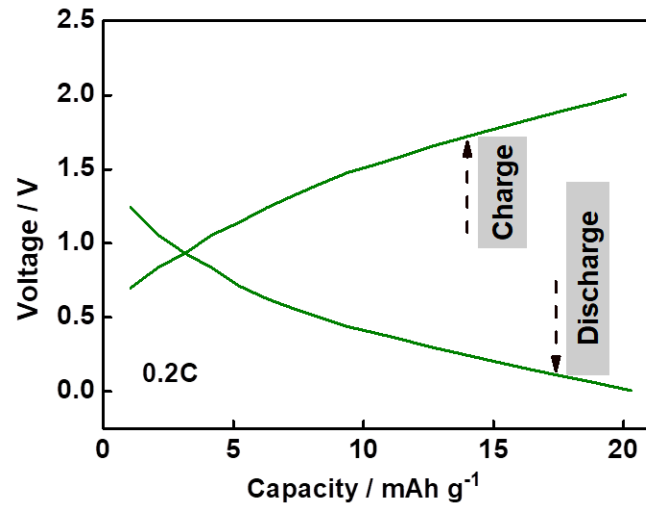


Fig. S6 Galvanostatic charge/discharge measurement (GCD) curve of HPC at a rate of 0.2C.

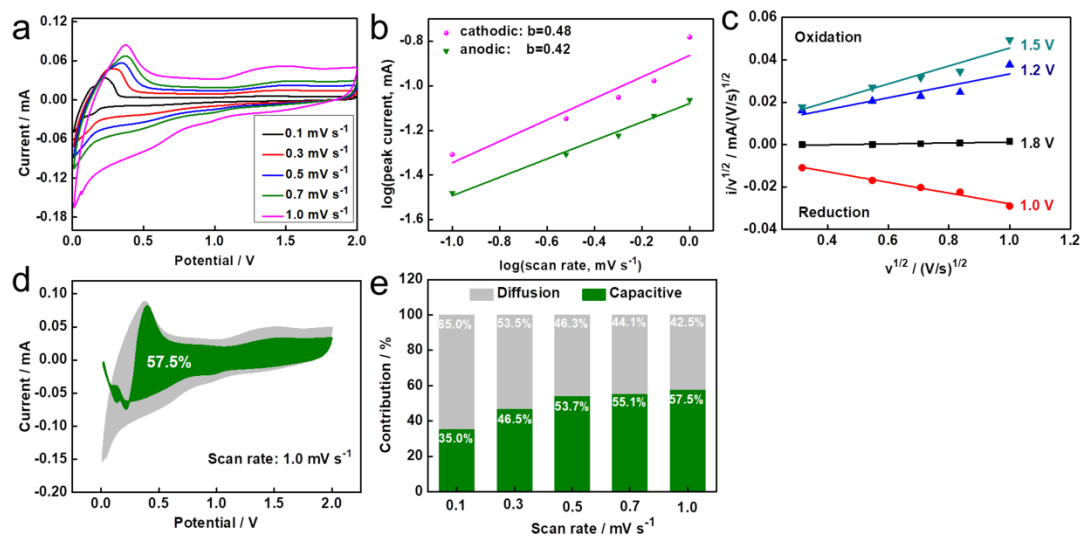


Fig. S7 (a) CV curves of graphite electrode at different scan rates from 0.1 to 1 mV s⁻¹. (b) Determination of b values using the relationship between the peak current and the scan rate. (c) Plots of $v^{1/2}$ vs. $i/v^{1/2}$ at different redox states for obtaining constants k_1 and k_2 , respectively. (d) The capacitive contribution at a scan rate of 1 mV s⁻¹. (e) Contribution ratio of the capacitive- and diffusion-controlled charge versus scan rate.

Supplementary method S1: Calculation of the capacitance contribution.

The current with scan rate in the CV test obeys the power law as below:

$$i = av^b \quad (1)$$

$$\log(i) = b \log(v) + \log a \quad (2)$$

where value b can be obtained from the slope of $\log(i)$ versus $\log(v)$ plot. Similarly, Equation (1) can be divided into two sections through the method proposed by Dunn and co-workers, as follows:

$$i = k_1 v + k_2 v^{1/2} \quad (3)$$

$$i/v^{1/2} = k_1 v^{1/2} + k_2 \quad (4)$$

where k_1 and k_2 are constants. The values of k_1 and k_2 can be obtained by the slope and intercept of $i/v^{1/2}$ versus $v^{1/2}$ plot, respectively. By applying k_1 and k_2 values at different voltages in $k_1 v$ and $k_2 v^{1/2}$, the capacitive and diffusion-controlled currents can be determined.